Article:
Zhang, M, Meng, W, Davies, TC et al. (2 more authors) (2016) A robot-driven computational model for estimating passive ankle torque with subject-specific adaptation. IEEE Transactions on Biomedical Engineering, 63 (4). pp. 814-821. ISSN 0018-9294

https://doi.org/10.1109/TBME.2015.2475161

A Robot-Driven Computational Model for Estimating Passive Ankle Torque with Subject-Specific Adaptation

Mingming Zhang, *Student Member, IEEE,* Wei Meng, T. Claire Davies, Yanxin Zhang, Sheng Q. Xie,* *Senior Member, IEEE*

***Abstract*— *Background*: Robot-assisted ankle assessment could potentially be conducted using sensor-based and model-based methods. Existing ankle rehabilitation robots usually use torquemeters and multi-axis load cells for measuring joint dynamics. These measurements are accurate, but the contribution as a result of muscles and ligaments is not taken into account. Some computational ankle models have been developed to evaluate ligament strain and joint torque. These models do not include muscles, and thus are not suitable for an overall ankle assessment in robot-assisted therapy. *Methods*: This study proposed a computational ankle model for use in robot-assisted therapy with three rotational degrees of freedom (DOFs), 12 muscles and seven ligaments. This model is driven by robotics, uses three independent position variables as inputs, and outputs an overall ankle assessment. Subject-specific adaptations by geometric and strength scaling were also made to allow for a universal model. *Results*: This model was evaluated using published results and experimental data from 11 participants. Results show a high accuracy in the evaluation of ligament neutral length and passive joint torque. The subject-specific adaptation performance is high, with each normalised root mean square deviation (NRMSD) value less than 10%. *Conclusion*: This model could be used for ankle assessment, especially in evaluating passive ankle torque, for a specific individual. The characteristic that is unique to this model is the use of three independent position variables that can be measured in real-time as inputs, which makes it advantageous over other models when combined with robot-assisted therapy.**

***Index Terms*—ankle assessment, computational model, robot-assisted therapy, robot-driven, subject-specific.**

I. Introduction

Robots have been developed for the treatment of various ankle injuries over the past decades. Wearable devices are usually aimed at ankle rehabilitation during gait exercises, while platform robots can only do ankle training [1-6]. Zhang, et al. [7] systematically reviewed various ankle rehabilitation devices and demonstrated their effectiveness in clinical applications. It was concluded that few existing robots conducted real-time ankle assessments to control the robot. The knowledge of ankle kinematics and dynamics may allow for the alteration of control strategies of robot-assisted therapy based on real-time ankle performance.

Ankle assessment is essential in robot-assisted therapy. Zhang, et al. [8] reviewed both qualitative and quantitative assessment techniques. They concluded that most quantitative assessment techniques are reliable in measuring ankle kinematics and dynamics, but are usually only available for the sagittal plane. Few studies conducted ankle assessments in a three-dimensional space where foot motion actually occurs [9]. Most ankle rehabilitation devices use torquemeters and multi-axis load cells for measuring joint dynamics [10, 11]. These measurements are accurate but expensive. Further assessment at the level of muscles and ligaments is also lacking, although Naito, et al. [12] conducted the identification of ankle muscle length using inverse kinematics.

Ankle assessment at the level of muscles and ligaments usually consists of cadaver-based sectioning studies [13, 14], invasive techniques [15] and image-based methods [16]. Cadaver-based and invasive methods are not suitable for rehabilitation. The high computation of image-based techniques limits their applications in real-time robotic environments. In a better way, some computational models have been developed for ankle assessment at the level of muscles and ligaments. Liacouras and Wayne [17] proposed a computational approach to model the lower leg to study syndesmotic injury and ankle inversion stability. This model simulated ligament sectioning experiments and actual foot motion was not fully represented. Lindner, et al. [18] created an ankle model, but with only lateral ankle ligaments included.

This work was supported by the University of Auckland under the Faculty of Engineering Research Development Fund 3625057 (Physical Robot-Human Interaction for Performance-Based Progressive Robot-Assisted Therapy) and the China Sponsorship Council. Ethics approval (9348) has been obtained from the University of Auckland Human Participants Ethics Committee.

M. M. Zhang is with the Department of Mechanical Engineering, University of Auckland, Auckland 1142, New Zealand (email: mzha130@aucklanduni.ac.nz).

W. Meng is with the Department of Mechanical Engineering, University of Auckland, Auckland 1142, New Zealand, and also with the School of Information Engineering, Wuhan University of Technology, Wuhan 430070, China (email: wmen386@aucklanduni.ac.nz).

T. C. Davies is with the Department of Mechanical Engineering, University of Auckland, Auckland 1142, New Zealand (email: c.davies@auckland.ac.nz).

Y. X. Zhang is with the Department of Sport and Exercise Science, University of Auckland, Auckland 1142, New Zealand (email: yanxin.zhang@auckland.ac.nz).

*S. Q. Xie is with the Department of Mechanical Engineering, University of Auckland, Auckland 1142, New Zealand (correspondence email: s.xie@auckland.ac.nz).

Wei, et al. [19] established a computational model for determining dynamic ankle ligament strains by inputing kinematic data from a six-camera Vicon MX Capture System. The issues of set-up and time-consuming analysis process impede its application in robot-assisted therapy. More recently, Wei, et al. [20] revised this model with three DOFs at two joints, in which the rotational axis of ankle inversion and eversion locates between the talus and the calcaneus. This model could provide ligament strains and joint moments but was only validated for ankle supination. In general, these evaluated models have been demonstrated to identify the kinematics and dynamics of the foot-ankle complex for some specific applications. However, these models do not include muscles and thus are not suitable for an overall ankle assessment in robot-assisted therapy.

The objective of this study was to develop and validate a novel computational ankle model for use in robot-assisted therapy. This robot-driven model uses three independent position variables as inputs while outputting an overall ankle assessment (kinematics and dynamics of ankle joint, muscles and ligaments). It was developed to allow for subject-specific results by scaling a general musculoskeletal model to enable the application to most of the population. This paper mainly focuses on the establishment of the ankle model, subject-specific adaptation and model validation.

II. Methods

A computational ankle model with three rotational DOFs and 19 force elements (FEs) was constructed for use in robot-assisted therapy. These 19 FEs consist of 12 muscles and seven ligaments. Subject-specific adaptations by geometric and strength scaling were made based on participants' height and weight to enable the application to most of the population. This robot-driven model considers three independent position variables as inputs, and outputs the kinematics and dynamics of individual muscle/ligament and the ankle joint, as shown in Fig. 1. Two significant assumptions are: 1) ankle motion exists at a single joint between the tibia/fibula unit and the talus/calcaneus. The tibia/ fibula is fixed during robot-assisted therapy while the talus/calcaneus rotates in three rotational DOFs; and 2) the rotational axes of ankle dorsiflexion/plantarflexion (DP), inversion/eversion (IE) and abduction/adduction (AA) intersect at one point to facilitate its use in robot-assisted therapy.

A. Model Formulation

This ankle model was created based on the lower extremity

TABLE I
POSITION/FORCE PARAMETERS OF MUSCLES AND LIGAMENTS

FE	Attachment location (mm)		ST or MF
	Origin	Insertion	
ATaFL^{+}	[3 -419 38]	[9 1 19]	90

TABLE II
PARTICIPANTS CHARACTERISTICS AND SCALING FACTORS

No.	Age	H	M	G-Scaling	S_1	BMI	S_2
1	23	173	80	[1.05,0.96, 1.05]	1.04	26.73	0.97
2	25	185	103	[1.16,1.03,1.16]	1.24	30.09	1.02
3	26	186	80	[1.02,1.03,1.02]	1.04	23.12	1.03
4	26	183	81	[1.03,1.02,1.03]	1.05	24.19	1.02
5	28	165	60	[0.93,0.92,0.93]	0.86	22.04	0.91
6	25	180	75	[1,1,1]	1	23.15	1
7^{f}	25	165	61	[0.94,0.92,0.94]	0.87	22.41	0.62
8^{f}	30	160	49	[0.86,0.89,0.86]	0.75	19.14	0.62
9^{f}	27	157	44	[0.82,0.87,0.82]	0.70	17.85	0.61
MRI	35	176	85	[1.08,0.98,1.08]			
MRI^{f}	27	166	51	[0.86,0.92,0.86]			

^{f} represents female participants and all others are males; No. represents participant number; Age (years), H (cm) is participant height and M (kg) refers to participant mass; BMI is the body mass index based on H and M; S_1 and S_2 represent two different strength scaling factors and they are defined in (5). MRI: Magnetic resonance imaging.

SOL	[-2 -153 7]	[0 31 -5]	3549
TIBANT	[33 -395 -18]	[117 18 -30]	905
TIBPOST	[-14 -405 -23]	[42 33 -29]	1588

ATaFL: Anterior talofilular ligament; PTaFL: Posterior talofibular ligament; ATiTL: Anterior tibiotalar ligament; PTiTL: Posterior tibiotalar ligament; CaFL: Calcaneofibular ligament; TiNL: Tibionavicular ligament; TiCL: Tibiocalcanean ligament; EXTDIG: Extensor digitorum longus; EXTHAL: Extensor hallucis longus; FLEXDIG: Flexor digitorum longus; FLEXHAL: Flexor hallucis longus; LATGAS: Lateral gastrocnemius; MEDGAS: Medial gastrocnemius; PERBREV: Peroneus brevis; PERLONG: Peroneus longus; PERTERT: Peroneus tertius; SOL: Soleus; TIBANT: Tibialis anterior; TIBPOST: Tibialis posterior; FE: Force element; ST: Stiffness; MF: Max force.

$^{+}$ represents FE insertion is relative to the talus coordinate system and all others are relative to the calcaneus coordinate system;

■ represents data from the lower extremity model;

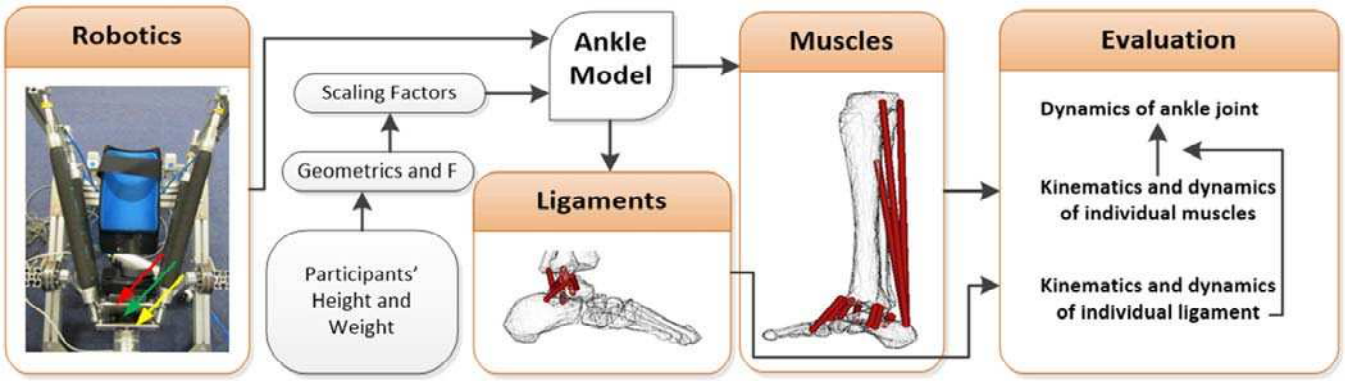

Fig. 1. A robotics-driven computational ankle model with muscles and ligaments for assessment with subject-specific adaptation. (The robot could drive this computational ankle model using three angular potentiometers around three rotational axes; the footplate denoted by the red arrow is fixed on the moving platform denoted by the yellow arrow by a six-axis load cell denoted by the green arrow (they comprise the end effector), and the moving platform with three rotational DOFs is driven by four parallel actuators).

model developed by Delp, et al. [21] in OpenSim [22] and analysed in MATLAB 2013b. The lower extremity model indicates DP at the ankle joint and IE at the subtalar joint. The AA was added in the proposed model for use in three-dimensional robot-assisted ankle therapy. These three rotational axes were modified in OpenSim to orthogonally intersect at a point considered as the rotation centre of the ankle-foot complex in robot-assisted therapy. Seven ligaments spanning this joint are included in the model and represented by linear elements. The corresponding attachment locations are determined from dissection and anatomical atlases [23, 24], as shown in Fig. 1 and Table I. Muscles included are the same as that in Gait2392 available open through to OpenSim source software [22], but only sections connecting the tibia/fibula and the talus/calcaneus are used, as shown in Fig. 1 and Table I. Ligament stiffness summarised by Wei, et al. [25] based on published data is used in this study and passive muscle force was calculated based on muscle length with respect to neutral length [26].

Definitions of the ankle coordinate system proposed by the Standardization and Terminology Committee of the International Society of Biomechanics were adopted in this model (with dorsiflexion, abduction and inversion defined as positive while plantarflexion, adduction and eversion defined as negative) [27]. Three coordinate frames respectively denoted as tibia/fibula, talus and calcaneus were defined to describe foot motions. The tibia/fibula frame xyz_{tib}, the talus frame xyz_{tal} and the calcaneus frame xyz_{cal} keep the same as that in the lower extremity model. xyz_{tib} is fixed and no movement exists between xyz_{tal} and xyz_{cal}. The coordinate of these attachment points described in xyz_{tib} could be obtained by translation based on ankle anatomy and rotation based on ankle motion, as shown in (1) and (2), where p represents the coordinate of the attachment point with respect to a certain coordinate frame, R is the rotation matrix depending on three independent angular variables denoted by θ_{dp}, θ_{ie} and θ_{aa}, and $T_{tia-tal}$ and $T_{tal-cal}$ are the translation matrices decided by ankle anatomy.

$$\begin{cases} p_{tib} = R \cdot p_{tal} + T_{tia-tal}, & FE\ \ at\ talus \\ p_{tib} = R \cdot [\![(p)]\!]_{tal} + T_{tal-cal}) + T_{tia-tal}, & FE\ at\ calcaneus \end{cases} \quad (1)$$

$$R = \begin{bmatrix} cos\theta_{aa}cos\theta_{ie} & R_{12} & R_{13} \\ sin\theta_{aa}cos\theta_{ie} & R_{22} & R_{23} \\ -sin\theta_{ie} & cos\theta_{ie}cos\theta_{dp} & cos\theta_{ie}cos\theta_{dp} \end{bmatrix},$$

$$\text{where} \begin{aligned} R_{12} &= -sin\theta_{aa}cos\theta_{dp} + cos\theta_{aa}sin\theta_{ie}sin\theta_{dp} \\ R_{13} &= sin\theta_{aa}sin\theta_{dp} + cos\theta_{aa}sin\theta_{ie}cos\theta_{dp} \\ R_{22} &= cos\theta_{aa}cos\theta_{dp} + sin\theta_{aa}sin\theta_{ie}sin\theta_{dp} \\ R_{23} &= cos\theta_{aa}cos\theta_{dp} + sin\theta_{aa}sin\theta_{ie}sin\theta_{dp} \end{aligned} \quad (2)$$

B. Subject-Specific Adaptation

This general model represents a young adult male with a height of 1.8 m and mass of 75 kg. Subject-specific adaptations in evaluating passive ankle torque were conducted on nine young adults (six males and three females) with age 26.11±2.03 years old, height 172.67±11.26 cm and weight 70.33±18.48 kg. Subject-specific adaptations in estimating ligament lengths were conducted on two additional adults (a male with age 35 years old, height 176 cm and weight 85 kg; and a female with age 27 years old, height 166 cm and weight 51 kg). Participants were required to have no history of severe ankle injuries, no acute ankle sprains within the last year, and no acute symptoms of pain or weakness. Table II summarises the characteristics of participants and scaling factors used in the proposed model.

The subject-specific adaptation used a non-uniform geometric scaling and mass-fat scaling defined by Rasmussen, et al. [28], see (3), (4) and (5). r and r_b represent actual coordinates and the base of FE attachment points. F and F_b represent actual force and the base of FEs. G is a 3 × 3 scaling matrix for segments, denoted by $G = diag[G_{11}, G_{22}, G_{33}]$, where $G_{11} = G_{33} = \sqrt{k_m/k_l}$, $G_{22} = k_l$, k_l and k_m represents height and weight ratio, the differences between S_1 and S_2 are if the fat-mass percentage is considered for strength scaling, R_{fat} is obtained based on (6) and R_{fat}^b is R_{fat} of the base model, and R_{other} is 0.5.

$$r = Gr_b \quad (3)$$

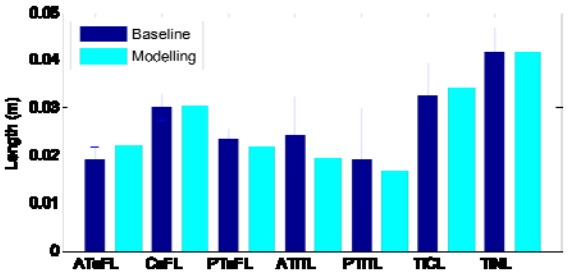

Fig. 2. Model-based neutral length and published length of ankle ligaments.

$$F = S_i F_b, \quad i = 1,2 \quad (4)$$

$$\begin{cases} S_1 = k_m^{2/3} \\ S_2 = \dfrac{k_m}{k_l}\dfrac{1 - R_{other} - R_{fat}}{1 - R_{other} - R_{fat}^b} \end{cases} \quad (5)$$

$$\begin{cases} R_{fat}^{men} = -0.09 + 0.0149 \cdot BMI - 0.00009 \cdot BMI^2 \\ R_{fat}^{women} = -0.08 + 0.0203 \cdot BMI - 0.000159 \cdot BMI^2 \end{cases} \quad (6)$$

C. Experimental Data

Experimental data regarding the relationship between ankle position and passive torque were collected by a manual ankle assessment device. This device mechanically consists of a handle for manual operation, a moving platform and a footplate rigidly fixed with an ankle orthosis. The components used for sensing include an angular potentiometer and a six-axis load cell (M3715C, Sunrise Instruments), which is the same as the end effector of 'Robotics' in Fig. 1. The rotational axis of the ankle orthosis was made to be consistent with that of the moving platform.

Participants were instructed to sit on a height-adjustable chair with the hip and knee joints in 90° of flexion. The ankle-foot complex was fixed onto the footplate by an ankle orthosis. The rotational axis of the ankle orthosis was visually adjusted to approximate the ankle joint. Participants were verbally encouraged to relax the foot-ankle complex to

minimise the effects by muscle activations. Extremes of ankle DP depended on the subjective sensation from participants until the foot is tense. The rotation was considered to be quasi-static with angular velocity less than 8°/s to reduce the effect by velocity. Five cycles (starting from neutral position defined as the ankle position where the foot and the leg are perpendicular to each other in sagittal plane based on [29], to extreme dorsiflexion, to neutral position, to extreme plantarflexion and getting back to neutral position) were conducted on each participant. This study was approved by the University of Auckland, Human Participants Ethics Committee (9348) for experimentation on human subjects, and consent was obtained from all participants. Data regarding the neutral lengths of ankle ligaments were obtained from two adults using MRI. The images were obtained using a Siemens Skyra 3T scanner and T1 weighted volume 0.6 x0.6 x 0.6 mm in a sagittal plane. The lengths of ankle ligaments were measured offline using syngo fastView.

D. Model Validation

Data based on the published literature [14, 16, 30-32] and passive torque collected from participants were used for model validation. The lengths of ankle ligaments depend on not only the bone geometry, but also their origin and insertion points on bones. An accurate ankle model should output accurate ligament lengths, and thus ligament lengths could be considered as a measure for model validation. Many researchers have investigated ligament lengths in the neutral position through either cadaver sectioning or image-based methods like MRI technique, as summarised in Table III. The summary means and standard deviations (SDs) were determined by meta-analysis using the Random Effect Model [33]. The experimental and modeling results were compared for each participant using mean average deviation (MAD), root mean square deviation (RMSD) and NRMSD for evaluating the subject-specific adaptation performance, as respectively shown in (7), (8) and (9). m_i and e_i represent modeling and experimental value at each selected step i, step refers to the moment for each data acquisition, and n is the total number of steps. Δ is the range of experimental values defined as the difference between the maximum and the minimum values in a data set.

$$MAD = \sum_{i=1}^{n} |m_i - e_i|/n \tag{7}$$

$$RMSD = \sqrt{\sum_{i=1}^{n} (m_i - e_i)^2/n} \tag{8}$$

$$NRMSD = \frac{RMSD}{\Delta} \times 100\% \tag{9}$$

III. Results

A. Neutral Ligament Length

Muscle and ligament length for any ankle position is assumed to be obtained from this computational model. Fig. 2 compares the model-based neutral ligament length with published data summarised in Table III. It was found that modeling results were reasonable and to some extent verify the effectiveness of this model.

B. Passive Ankle Torque

Ankle torque could be divided into passive torque and active torque. Passive ankle torque was calculated and compared with experimental results. Muscles' active contribution to ankle dynamics is not in the interest of this study. Fig. 3 plots the total passive ankle torque in DP, and contributions by muscles and ligaments are also presented separately. Individual FE force distributions with ankle position can be seen from Figs. 3, 4 and 5. Fig. 6 describes passive ankle torque in IE (above) and AA (below), respectively. Passive joint torque at maximum inversion was compared well with published data [34] and no published data regarding the torque evaluation for ankle AA.

The general model used in this study got the similar characteristics (gender, age, height and weight) as participant No. 6. Thus a direct comparison between modeling results and experimental data on participant No. 6 was conducted to validate the effectiveness of this model. To facilitate the comparison, data processing was conducted over five trials on each participant to eliminate random errors caused by participants and the manual operation, see Fig. 7. The curve in cyan is considered as the baseline for model evaluation. Fig. 8 shows the direct comparison between modeling results and experimental data on participant No. 6. MAD, RMSD and NRMSD are 0.4926, 0.5326 and 3.0034%, respectively. The individual contribution of each FE is clearly presented.

C. Subject-Specific Adaptation Performance

This model was mainly developed to be subject-specific in evaluating passive ankle torque based on participants' height and weight by two scaling (geometric and strength) factors. Comparison curves on each participant are shown in Fig. 9 and statistical data are summarised in Table IV. MAD values are less than 1 Nm, except for the one using S1 on participant No. 2. RMSD values are less than 1 Nm, except for the one using S1

TABLE III
Published Neutral Lengths of Ankle Ligaments

Studies	Length / mm (*Means ±S Ds*)							
	ATaFL	**CaFL**	**PTaFL**	**ATiTL**	**PTiTL**	**TiCL**	**TiNL**	**S S**
Siegler et al. [30]	17.81±3.05	27.69±3.30	21.16±3.86	—	11.86±3.96	—	41.83±4.93	20
Ozeki et al. [14]	19.80±1.92	29.9±4.24	23.70+3.10	—	—	27.7±3.76	—	12
Mkandawire et al. [31]	18.89±2.97*	35.44±6.31	27.74±3.41	24.09±8.03	26.68±4.49	37.45±2.74	—	6
Taser et al. [32]	22.37±2.50	31.94±3.68	21.66±4.84	—	—	—	—	42
Asla et al. [16]	16.30±3.0	28.00±2.90	—	—	—	—		4
Combined	***19.22±2.50***	***30.19±2.74***	***23.35±2.38***	***19.18±10.48***	***15.28±7.52***	***32.44±6.89***	***41.83±4.93***	—

* represents the sample size is 5, SS represents sample size and values in bold and italic represent the reliable results that would be regarded as the baseline for the validation of this model.

TABLE IV
SUBJECT-SPECIFIC ADAPTATION PERFORMANCE ON ESTIMATION OF PASSIVE ANKLE TORQUE OF NINE PARTICIPANTS

No.	MAD (Nm)			RMSD (Nm)			NRMSD (%)		
	NS	S_1	S_2	NS	S_1	S_2	NS	S_1	S_2
1	0.5173	0.8531	0.5318	0.5729	0.9613	0.6112	3.0611	5.1359	3.2653
2*	0.4583	1.8434	0.7377	0.7273	2.0734	0.8353	3.3946	9.6779	3.8990
3	0.4514	0.4848	0.4683	0.7366	0.5998	0.6006	3.2437	2.6415	2.6448
4	0.4387	0.4202	0.4310	0.5041	0.5307	0.4627	2.4858	2.6170	2.2816
5	1.6334	0.5402	0.6540	2.0202	0.7462	0.9252	13.8287	5.1080	6.3336
6		0.4926			0.5326			3.0034	
7f	1.6596	0.6289	0.7834	2.0213	0.7603	0.9557	14.7807	5.5600	6.9888
8f	2.3698	0.3858	0.2542	2.7863	0.4587	0.2862	26.7397	4.4022	2.7465
9f	2.1983	0.4176	0.7467	2.6193	0.5538	0.9223	19.6852	4.1617	6.9317

TABLE V
SUBJECT-SPECIFIC ADAPTATION PERFORMANCE ON TWO PARTICIPANTS

No. \ Ligament		Length / mm						
		ATaFL	PTaFL	ATiTL	PTiTL	CaFL	TiNL	TiCL
MRI	Modeling	23.6	23.2	19.9	16.5	32.2	43.5	33.3
	Measured	23.1	23.1	19.0	16.6	32.8	44.1	34.5
MRIf	Modeling	19.4	19.0	17.3	15.4	26.6	37.1	31.4
	Measured	19.2	19.2	17.7	15.5	26.1	37.6	31.4

on participant No. 2 and the ones using S2 on three female participants. All NRMSD values are less than 10%. To present the significance of subject-specific adaptation, statistical results with no scaling (NS) are also included in Table IV. The results from participant No's. 1, 2, 3, 4 and 6 present good modeling accuracy with all NRMSD values less than 4%, while those from participant No's. 5, 7, 8 and 9 do not with all NRMSD values greater than 13.8%.

The evaluation of passive ankle torque correlates with the ligament lengths. The performance of the subject-specific adaptation in evaluating ligament lengths is presented in Table V, where the model-based neutral length of each ligament compares well with that from MRI data with all differences less than 1 mm.

IV. DISCUSSION

The potential of this model for use in robot-assisted ankle therapy is discussed first. The required kinematic inputs to existing computational models are usually obtained from marker-based motion capture systems [35]. This motion analysis technique is not convenient when combined with robot-assisted therapy due to the issues of set-up and time-consuming analysis. The required inputs to the model are three independent position variables that could be easily sensed from existing ankle

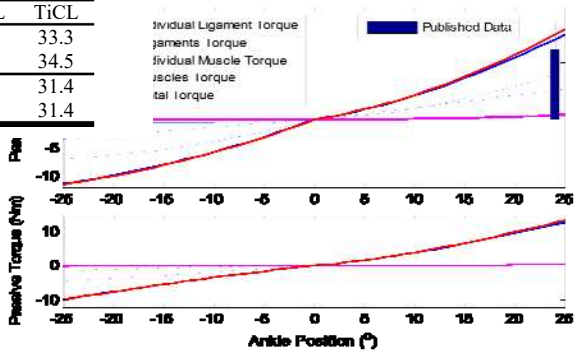

Fig. 6. Model-based passive joint torque in ankle IE (above) and AA (below).

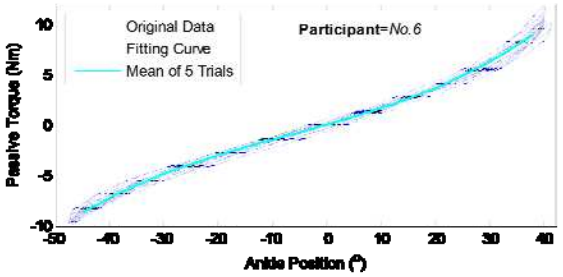

Fig. 7. Experimental passive ankle DP torque over five tests on participant No. 6.

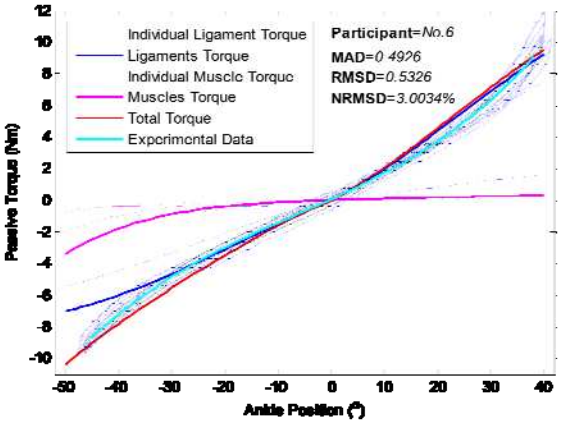

Fig. 8. Comparison between modeling results and experimental data on participant No. 6.

rehabilitation robots. The devices described in [3, 4] represent two typical ankle rehabilitation robots, with or without physical rotational axes of end effectors. Both can use linear potentiometers to evaluate the posture of the end effect using forward kinematics or only a multi-axis inclinometer. An alternative method for robots with physical axes is to use angular potentiometers. In general, the required inputs to this model could be easily obtained from robotic devices, which provide the basis for use in robot-assisted ankle therapy.

Existing computational ankle models are usually developed for ligament analysis for certain specific applications. The overall ankle joint torque could not be reliably evaluated without considering the contribution of muscles. However, this proposed ankle model could be used for evaluating ankle joint torque by computing the contribution of each FE. The use of this ankle model may permit a less expensive rehabilitation system, for example by replacing the need to use expensive sensors. Improvement regarding the robotic design for ankle therapy could be further achieved, although a range of robot-assisted ankle rehabilitation techniques have been demonstrated to be effective for individuals with ankle injuries [7]. This model could be used for robot-assisted ankle assessment at the level of joint and FEs.

The model structure is different with ankle anatomy and published models with ankle joint between the tibia/fibula and the talus and subtalar joint between the talus and the calcaneus [21, 36]. Siegler, et al. [37] concluded that DP mainly exists at the ankle joint, IE mainly exists at the subtalar joint, and other motion could be the combination of the ankle joint and the subtalar joint. The DP axis in the proposed model can be approximately considered to be consistent with ankle anatomy, while the IE and AA axes are obviously different with ankle anatomy. Thus direct comparison between modeling results and published data, mainly in terms of ankle DP, was conducted for model evaluation. Fig. 6 shows passive ankle torque in IE (above) and AA (below), respectively, where the passive joint torque in extreme inversion was well compared with published data [34] on subjects with recurrent ankle inversion sprains, although the maximum positions were not completely consistent.

For model evaluation in DP, both the neutral ligament length and passive joint torque are considered as the measures. The measured ankle ROM (-50° of plantarflexion and 40° of dorsiflexion) is considered to be reasonable with high driving torque applied, which is verified by a physiotherapy expert. Comparisons with published neutral ligament lengths obtained from cadaver anatomy and MRI were conducted. In Fig. 2, the neutral ligament length calculated from this computational model shows satisfactory accuracy by comparing with published data. The main purpose of this model is to evaluate passive joint torque as foot moves for use in robot-assisted therapy. Modeling results were compared with experimental data on participant No. 6 in Fig. 8 and a high accuracy was achieved, with MAD, RMSD and NRMSD values being 0.4926, 0.5326 and 3.0034%, respectively. The contribution of individual FE, as shown in Figs. 4 and 5, is not validated in this study since no published evidence has been found. Subject-specific adaptations by geometric and strength scaling were made in this model.

Comparisons were conducted on each participant and results show a satisfactory accuracy, with each NRMSD value less than 10%. However, the accuracies vary for different participants, as shown in Fig. 9 and Table IV, which could be caused by various factors like age and gender [38, 39]. Most subject-specific performance on males is close with different strength scaling factors. Strength scaling using S1 on participant No. 2 presents less accuracy than that with S2 and the reason could be that S1 does not consider the influence from

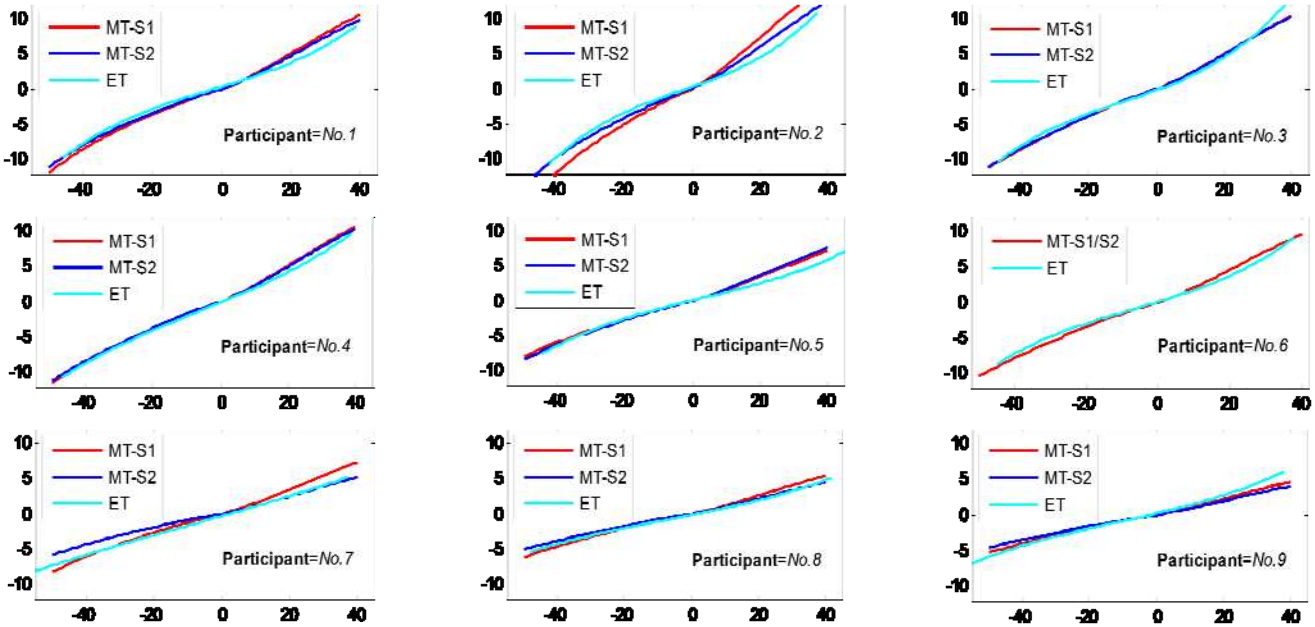

Fig. 9. Comparison curves between modeling results and experimental data on nine participants (MT-S1: Modeling torque using S1; MT-S2: Modeling torque using S2; ET: Experimental torque; X-coordinate is ankle position in DP /°; Y-coordinate is passive ankle torque /Nm).

the fat percent. However, the subject-specific performance on participants with moderate BMI values presents better estimation accuracy. NRMSD values on participants No's. 3, 4 and 8 using S2 are less than 3%.

To present the significance of the subject-specific adaptation, the accuracy in evaluating passive ankle torque with respect to NS is also analysed and presented in Table IV. There are significant differences among these nine participants regarding the model-based prediction accuracy with NS. The data from participant No's. 1, 2, 3, 4 and 6 are encouraging, while those from participant No's. 5, 7, 8 and 9 do not show satisfactory prediction accuracy. The potential reason is that the base model used in this study represents a young adult male with a height of 1.8 m and mass of 75 kg, which is closer to those of participant No's. 1, 2, 3, 4 and 6 than others. Further, it can be seen that the subject-specific adaptation seems more necessary for female subjects than males, which is clearly presented in Table IV where the torque estimation with subject-specific adaptation present significantly improved accuracy with the NRMSD values being 14.7807%, 26.7397% and 19.6852% for participant No's 7, 8 and 9 with respect to all less than 7% without NS. The reason could be the gender and the body size differences of these three females as the base model. Another interesting point is that estimation with NS is successful and achieves better results than "subject-specific adaptation" method for participant No's 1, 2 and 4. This behaves abnormal since the subject-specific adaptation does not improve the model based estimation as expected, from the other hand this is normal because the estimation accuracy has been high with all NRMSD values less than 3.5% when with NS. In general, subject-specific adaptation does not contribute significantly once a high-precision estimation (<10%) has been obtained. However, a more comprehensive subject-specific adaptation law should be investigated in near future with body size, gender, age, health condition, and even ethnic group all considered.

Some other limitations of the model should be also noted. The linear representation of muscles and ligaments as being straight lines between origin and insertion points may affect the estimation of joint torque. The subject-specific adaptation was conducted based on participants' height and weight, and factors like gender, age and health condition should be also included for future improvement. An alternative scaling method can be made based on foot geometry instead of body height and weight. This model assumed normal elastic properties of the ligaments and muscles and thus could reliably predict passive ankle torque for healthy subjects. However, the prediction could be inaccurate (due to abnormal muscle and ligament property) if the robotic training is delivered to ankle impaired subjects. For example, some pathological conditions have not just stiffer ligaments, but shortened ones. Further improvement will take patients' health condition into consideration for subject-specific adaption. Although this model can quantify the individual contribution of ankle muscles and ligaments, the estimation accuracy was not validated experimentally. Published data in this field are also limited.

V. Conclusion

This three-DOF computational ankle model with muscles and ligaments was developed for use in robot-assisted therapy. The use of three independent position variables required as inputs offers an advantage over other models when combined with robot-assisted therapy. This model could evaluate passive ankle torque in DP, IE and AA in robot-assisted therapy for a specific subject, as well as the individual contribution of ankle muscles and ligaments. The information could be helpful for designing a patient-specific therapy program and have more advantages than conventional functional assessment. Future studies could further generalise this model by: 1) incorporating muscles' active contribution; and 2) scaling the strength of muscles and ligaments based on the health condition of patients.

Acknowledgment

This material was supported by the University of Auckland, Faculty of Engineering Research Development Fund 3625057 and the China Sponsorship Council. The authors also thank Dr John Parsons in verifying the measured ROM of ankle plantarflexion and dorsiflexion, and Professor Allan Chang in summarizing data form different sources.

References

[1] A. Roy, H. I. Krebs, D. J. Williams, C. T. Bever, et al., "Robot-Aided Neurorehabilitation: A Novel Robot for Ankle Rehabilitation," *IEEE Transactions on Robotics*, vol. 25, pp. 569-582, 2009.

[2] L. W. Forrester, A. Roy, H. I. Krebs, and R. F. Macko, "Ankle Training With a Robotic Device Improves Hemiparetic Gait After a Stroke," *Neurorehabilitation and Neural Repair*, vol. 25, pp. 369-377, May 2011.

[3] Y. H. Tsoi and S. Q. Xie, "Design and control of a parallel robot for ankle rehabilitation," *International Journal of Intelligent Systems Technologies and Applications*, vol. 8, pp. 100-113, 2010.

[4] P. K. Jamwal, S. Q. Xie, S. Hussain, and J. G. Parsons, " An Adaptive Wearable Parallel Robot for Ankle Injury Treatments," *IEEE Transactions on Mechatronics*, vol. 19, pp. 64-75, 2014.

[5] Y. L. Park, B. R. Chen, N. O. Pérez-Arancibia, D. Young, L. Stirling, R. J. Wood, E. C. Goldfield, and R. Nagpal, "Design and control of a bio-inspired soft wearable robotic device for ankle-foot rehabilitation," *Bioinspiration and Biomimetics*, vol. 9, 2014.

[6] H. Yu, S. Huang, G. Chen, and N. Thakor, "Control design of a novel compliant actuator for rehabilitation robots," *Mechatronics*, vol. 23, pp. 1072-1083, 2013.

[7] M. Zhang, T. C. Davies, and S. Xie, "Effectiveness of robot-assisted therapy on ankle rehabilitation -- a systematic review," *J Neuroeng Rehabil*, vol. 10, p. 30, Mar 21 2013.

[8] M. Zhang, T. C. Davies, Y. Zhang, and S. Xie, "Reviewing effectiveness of ankle assessment techniques for use in robot-assisted therapy," *Journal of Rehabilitation Research & Development*, vol. 51, 2014.

[9] G. J. Sammarco, *Rehabilitation of the Foot and Ankle.* Missouri, USA: Mosby-Year Book, 1995.

[10] Q. Peng, H.-S. Park, P. Shah, N. Wilson, Y. Ren, et al., "Quantitative evaluations of ankle spasticity and stiffness in neurological disorders using manual spasticity evaluator," *Journal of Rehabilitation Research and Development*, vol. 48, p. 473, 2011.

[11] J. A. Saglia, N. G. Tsagarakis, J. S. Dai, and D. G. Caldwell, "Control Strategies for Patient-Assisted Training Using the Ankle Rehabilitation Robot (ARBOT)," *IEEE/ASME Transactions on Mechatronics*, vol. 18, pp. 1799-1808, 2013.

[12] H. Naito, Y. Akazawa, A. Miura, T. Matsumoto, and M. Tanaka, "Identification of individual muscle length parameters from measurements of passive joint moment around the ankle joint," *Journal of Biomechanical Science and Engineering*, vol. 7, pp. 168-176, 2012.

[13] M. R. Colville, R. A. Marder, J. J. Boyle, and B. Zarins, "Strain measurement in lateral ankle ligaments," *The American Journal of Sports Medicine*, vol. 18, pp. 196-200, 1990.
[14] S. Ozeki, K. Yasuda, K. Kaneda, K. Yamakoshi, and T. Yamanoi, "Simultaneous Strain Measurement With Determination of a Zero Strain Reference for the Medial and Lateral Ligaments of the Ankle " *Foot & Ankle International*, vol. 23, pp. 825-832, 2002.
[15] B. D. Beynnon, B. C. Fleming, R. J. Johnson, C. E. Nichols, P. A. Renström, and M. H. Pope, "Anterior Cruciate Ligament Strain Behavior During Rehabilitation Exercises In Vivo," *The American Journal of Sports Medicine*, vol. 23, pp. 24-34, 1995.
[16] R. J. d. Asla, M. Kozanek, L. Wan, H. E. Rubash, and G. Li, "Function of anterior talofibular and calcaneofibular ligaments during in-vivo motion of the ankle joint complex," *Journal of Orthopaedic Surgery and Research*, vol. 4:7, 2009.
[17] P. C. Liacouras and J. S. Wayne, "Computational modeling to predict mechanical function of joints: application to the lower leg with simulation of two cadaver studies," *Journal of Biomechanical Engineering*, vol. 129, pp. 811-817, 2007.
[18] M. Lindner, A. Kotschwar, R. R. Zsoldos, M. Groesel, and C. Peham, "The jump shot – A biomechanical analysis focused on lateral ankle ligaments," *Journal of Biomechanics*, vol. 45, pp. 202-206, 2012.
[19] F. Wei, J. E. Braman, B. T. Weaver, and R. C. Haut, "Determination of dynamic ankle ligament strains from a computational model driven by motion analysis based kinematic data," *Journal of Biomechanics*, vol. 44, pp. 2636-2641, 2011.
[20] F. Wei, D. T.-P. Fong, K.-M. Chang, and R. C. Haut, "Estimation of ligament strains and joint moments in the ankle during a supination sprain injury," *Computer Methods in Biomechanics and Biomedical Engineering*, 2013.
[21] S. L. Delp, J. P. Loan, M. G. Hoy, F. E. Zajac, E. L. Topp, and J. M. Rosen, "An interactive graphics-based model of the lower extremity to study orthopaedic surgical procedures," *IEEE Transactions on Biomedical Engineering*, vol. 37, pp. 757-767, 1990.
[22] S. L. Delp, F. C. Anderson, A. S. Arnold, P. Loan, A. Habib, C. T. John, E. Guendelman, and D. Thelen, "OpenSim: Open-Source Software to Create and Analyze Dynamic Simulations of Movement," *IEEE Transactions on Biomedical Engineering*, vol. 54, pp. 1940-1950, 2007.
[23] P. Golano, J. Vega, P. A. de Leeuw, F. Malagelada, M. C. Manzanares, V. Gotzens, and C. N. van Dijk, "Anatomy of the ankle ligaments: a pictorial essay," *Knee Surgery, Sports Traumatology, Arthroscopy*, vol. 18, pp. 557-69, May 2010.
[24] B. M. Logan and R. T. Hutchings, *McMinn's color atlas of foot and ankle anatomy*, 3rd ed.: Elsevier, 2012.
[25] F. Wei, S. C. Hunley, J. W. Powell, and R. C. Haut, "Development and Validation of a Computational Model to Study the Effect of Foot Constraint on Ankle Injury due to External Rotation," *Annals of biomedical engineering* vol. 39, pp. 756-765 2011.
[26] K. HASE and N. YAMAZAKI, "Development of Three-Diemnsional Whole-Body Musculoskeletal Model for Various Motion Analyses," *JSME international journal. Ser. C, Dynamics, control, robotics, design and manufacturing*, vol. 40, pp. 25-32, 1997.
[27] G. Wu, S. Siegler, P. Allard, C. Kirtley, A. Leardini, D. Rosenbaum, M. Whittle, D. D. D'Lima, L. Cristofolini, H. Witte, O. Schmid, and I. Stokes, "ISB recommendation on definitions of joint coordinate system of various joints for the reporting of human joint motion—part I: ankle, hip, and spine," *Journal of Biomechanics*, vol. 35, pp. 543-548, 2002.
[28] J. Rasmussen, M. d. Zee, M. Damsgaard, S. T. Christensen, C. Marek, and K. Siebertz, "A General Method for Scaling Musculo-Skeletal Models," in *International Symposium on Computer Simulation in Biomechanics*, Cleveland, Ohio, United States, 2005.
[29] P. S. Sung, J.-Y. Baek, and Y. H. Kim, "Reliability of the intelligent stretching device for ankle stiffness measurements in healthy individuals," *Foot*, vol. 20, pp. 126-32, 2010.
[30] S. Siegler, J. Block, and C. D. Schneck, "The Mechanical Characteristics of the Collateral Ligaments of the Human Ankle Joint," *Foot & Ankle International*, vol. 8, pp. 234-242 1988.
[31] C. Mkandawire, W. Ledoux, B. Sangeorzan, R. Ching, "Foot and ankle ligament morphometry," *J Rehabil Res Dev*, vol. 42, pp. 809-820, 2005.
[32] F. Taser, Q. Shafiq, and N. A. Ebraheim, "Anatomy of lateral ankle ligaments and their relationship to bony landmarks," *Surgical And Radiologic Anatomy*, vol. 28, pp. 391-7, Aug 2006.
[33] Computer Program for Meta-Analysis. Heterogeneity, Publication Bias, and Combining Effect Sizes. [Online] Available: https://www.statstodo.com/MetaAnalysis_Pgm.php
[34] T. Birmingham, B. Chesworth, H. Hartsell, A. Stevenson, G. Lapenskie, and A. Vandervoort, "Peak Passive Resistive Torque at Maximum Inversion Range of Motion in Subjects With Recurrent Ankle Inversion Sprains," *Journal Of Orthopaedic & Sports Physical Therapy*, vol. 25, pp. 342-348, 1997/05/01 1997.
[35] T. W. Lu and J. J. O'Connor, "Bone position estimation from skin marker co-ordinates using global optimisation with joint constraints," *Journal of Biomechanics*, vol. 32, pp. 129-134, 1999.
[36] R. E. Isman and V. T. Inman, "Anthropometric studies of the human foot and ankle," *Bull Prosth Res*, vol. 11, pp. 97-129, 1969.
[37] S. Siegler, J. Chen, and C. D. Schneck, "The Three-Dimensional Kinematics and Flexibility Characteristics of the Human Ankle and Subtalar Joints—Part I Kinematics1," *Journal of Biomechanical Engineering*, vol. 110, pp. 364-373, 1988.
[38] D. G. Thelen, "Adjustment of muscle mechanics model parameters to simulate dynamic contractions in older adults," *Journal of Biomechanical Engineering*, vol. 125, pp. 70-77, 2003.
[39] S. D'Souza, J. Rasmussen, and A. Schwirtz, "Multiple linear regression to develop strength scaled equations for knee and elbow joints based on age, gender and segment mass," *International Journal of Human Factors Modelling and Simulation*, vol. 3, pp. 32-47, 2012.